THE JOURNAL OF PHYSICAL CHEMISTRY A

Article

pubs.acs.org/JPCA

Vibrational Anharmonicities and Reactivity of Tetrafluoroethylene

Werner Fuß,*[,†,&] Evan G. Robertson,*[,‡] Chris Medcraft,[§,⊥] and Dominique R. T. Appadoo[∥]

[†]Max-Planck-Institut für Quantenoptik, 85748 Garching, Germany

[‡]Department of Chemistry, La Trobe Institute of Molecular Sciences, La Trobe University, Bundoora, Victoria 3086, Australia

[§]School of Chemistry, Monash University, Wellington Road, Clayton, Victoria 3800, Australia

[∥]Australian Synchrotron, 800 Blackburn Road, Clayton, Victoria 3168, Australia

Supporting Information

ABSTRACT: Compared to ethylene and its nonfluorinated derivatives, C_2F_4 is peculiar in many reactions. It very easily adds to radicals and prefers formation of four-membered rings over Diels–Alder reactions. This has been rationalized by the preference of fluorine for carbon sp^3 hybridization, which is possible on opening of the double bond. Another property, the thermal dissociation of the C=C bond, has been explained by the stabilization of the product (CF_2) by back-bonding. Here, it is attempted to correlate such properties with vibrational constants, in particular for C=C stretching and twisting and for carbon pyramidalization. The only force constant found to be lowered compared to ethylene is that for trans pyramidalization (ν_8), and CC bond softening on ν_8 distortion is indicated by the conspicuously large magnitude of anharmonic constant, x_{18}. Both observations can be rationalized by a valence-bond model that predicts a trans bent structure on weakening the CC bond. Conclusions are drawn about the dissociation path and peculiarities of the potential. Other anharmonicities, both experimental and calculated and some in $^{12}C^{13}CF_4$ and $^{13}C_2F_4$, are also discussed. In particular some strong Fermi resonances are identified and their effects accounted for.

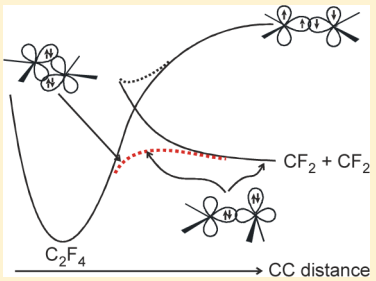

1. INTRODUCTION

Recently we reported on an analysis of the infrared spectrum of C_2F_4.[1] By observation of many combination and difference bands, including many from two ^{13}C-containing isotopologues, and by comparison with MP2 and density-functional calculations, all 12 fundamentals could be assigned, although only five are IR active. The necessary anharmonic corrections were derived from hot bands and combination bands. The focus was on deriving spectroscopic constants and on structural aspects. The geometry was deduced from ro-vibrational analysis of strong IR active bands and by comparison with theoretical calculations. However, it is also instructive to correlate anharmonic constants with some peculiarities of the reactions of C_2F_4. Accordingly, in this work more anharmonic constants (altogether 54) are derived from the spectra, and a complete set (78) is calculated. The earlier vibrational assignments of C_2F_4 were reported at a time when the unusual properties of this molecule were barely known.[2−5]

C_2F_4 very easily adds radicals. Borden et al. explained this property by positing that the electron attraction of fluorine leads to a preference of sp^3- over sp^2-type carbon:[6,7] Radical addition converts both C atoms from sp^2 to sp^3 hybridization, which stabilizes the primary product, lowers the transition state, and thus accelerates the reaction. C_2F_4 also prefers [2 + 2]-cycloaddition over Diels–Alder reactions, for example, which was again explained by stabilization of radical intermediates.[6,7] (Borden also presented an alternative but related description based on delocalization of unpaired radicalic electrons to accepting σ^* orbitals of CF groups.[7]) The preference for carbon sp^3 hybridization can also be expected to lower the force constants for the pyramidalization (wagging) vibrations (ν_7, ν_8) and/or increase their anharmonicity. Furthermore, torsion (ν_4) should be facilitated by rehybridization and in fact quantum chemistry confirmed this for a 90° twist.[8] The present work reveals finer aspects, however.

Another spectacular property of C_2F_4 is how readily it can dissociate thermally to two CF_2 molecules.[9,10] A C=C bond energy of only 2.95 eV is derived,[10] less than that of a typical C–C single bond (4 eV). The low dissociation energy is caused by stabilization of the resulting two difluorocarbenes by back-bonding from nonbonding fluorine electrons to the empty carbon p-orbital.[8,11−13] This also explains why CF_2 has a singlet ground state which is more stable than the triplet (by 2.458 eV, taken from the band origin of the phosphorescence spectrum[14,15]). Whereas in the previous work, only CC stretching is considered as the dissociation coordinate, it was argued in ref 16 that pyramidalization must also be involved. This idea is supported in the present work by the large value found for the anharmonic constant x_{18} coupling CC stretch with trans pyramidalization. The magnitude of x_{18} as compared to the much smaller x_{17} (coupling CC stretch with cis pyramidalization) also supports a valence-bond analysis of weak double bonds,[12,13,17,18] which was reviewed in ref 19.

Received: January 23, 2014
Revised: May 20, 2014
Published: June 4, 2014

   dx.doi.org/10.1021/jp500811w | J. Phys. Chem. A 2014, 118, 5391−5399

2. METHODS

The samples in natural isotopic abundance were either taken from commercial C_2F_4 (Hoechst), that contained a trace of the cyclic dimer, or prepared[20] from $C_2F_4Br_2$ + Zn in a high-boiling alcohol (diethylene glycol); the comparison allowed for recognizing absorptions of impurities. A sample enriched in ^{13}C to 50% was prepared from $CHClF_2$ by CO_2 laser isotope separation with enriched CF_2 as the primary product.[21] The dimerization product C_2F_4 was separated from $CHClF_2$ by low-temperature distillation.[1,21]

IR spectra of C_2F_4 in natural isotopic abundance and isotopically enriched were recorded between 370 and 4000 cm^{-1} with 0.2 cm^{-1} resolution by a PerkinElmer FTIR spectrometer in Garching.[1] At the Synchrotron lab, the isotopically enriched sample was measured at moderate 0.1 cm^{-1} resolution in the far IR region from 100 to 600 cm^{-1} (capturing the band at 210 cm^{-1}), and at high resolution for the IR active CF stretch bands, see ref 1. The present work focuses on anharmonic constants of $^{12}C_2F_4$. Only where the constants were expected to be different for $^{12}C^{13}CF_4$ and $^{13}C_2F_4$ (e.g., in the case of Fermi resonance) were the bands for these isotopologues evaluated to recover the corresponding constants. For the fundamentals and their isotopic shifts, see ref 1.

Theoretical values of the anharmonic constants x_{ij} were obtained from anharmonic vibrational frequency calculations performed using *Gaussian 03* Revision C02[22] at the MP2 level using Dunning-type correlation-consistent (cc-pVTZ) orbitals.[23] The molecular force field at this level of theory was shown in the previous study to reproduce the fundamental wavenumbers and the isotopic shifts of C_2F_4 very satisfactorily (for details, see ref 1), and hence was an appropriate choice for computing x_{ij} values. The calculations were performed for each of the $^{12}C_2F_4$, $^{12}C^{13}CF_4$, and $^{13}C_2F_4$ isotopologues.

3. RESULTS

The spectra were measured previously and the fundamentals extracted from them, using a limited number of anharmonic constants (from combination and hot bands) where necessary.[1] For convenience Table 1 lists the fundamentals again. In this work we derived a large set of experimental anharmonic constants from combination bands and—in particular for the lower-wavenumber vibrations—from hot bands, and report a complete set of theoretically computed values. They are compared in Table 2(see also Scheme 1).

The anharmonic constants x_{ij} were calculated from observed combination and difference bands by assuming that anharmonic shifts are additive: For binary combination bands ($i \neq j$) and for overtones we used

$$(\nu_i + \nu_j) = \nu_i + \nu_j + x_{ij} \quad (1)$$

and

$$(v_i\nu_i) = v_i\nu_i + v_i(v_i - 1)x_{ii} \quad (2)$$

with obvious extensions for more complicated combinations. (The x_{ij} values are mostly negative, as usual.) The left-hand side of these equations should be read as "wavenumber of (*name*)". For hot bands (satellite transitions near ν_i that originate from a thermally populated lower level ν_j) we used

$$(\nu_i + \nu_j) - \nu_j = \nu_i + x_{ij} \text{ (or } 2x_{ij}, \text{ if } i = j) \quad (3)$$

again with obvious extensions. One can often observe sequences of equidistant Q branches, corresponding to hot bands starting from higher levels $m\nu_j$, or combination of such sequences (from $m\nu_j + n\nu_k$). Equation 3 implies that the distance of a (first) hot band from the fundamental directly indicates the corresponding anharmonic constant. Combination bands allow for a direct assignment, whereas hot bands must be identified by their intensity (controlled by the Boltzmann factor). In a number of cases, the anharmonic constants resulted from both combination and hot bands. The Supporting Information (SI) compiles the sources for each x_{ij} in Table S2, whereas Table S1 lists the observed bands (with hot bands) and their isotopic shifts. Two examples of hot bands, whose shifts are dominated by the large x_{18} anharmonicity, are shown in Figure 1.

Table 1. Fundamentals of $^{12}C_2F_4$ (experimental wavenumbers in cm^{-1})[1]

mode	description	symmetry[a]	wavenumber
ν_1	C=C stretch	a_g (a_g)	1873.8
ν_2	CF_2 sym stretch	a_g (a_g)	776.1
ν_3	CF_2 scissor	a_g (a_g)	395.1
ν_4	CF_2 twist	a_u (a_u)	193.7
ν_5	CF_2 asym stretch	b_{2g} (b_{1g})	1337.7
ν_6	CF_2 rock	b_{2g} (b_{1g})	550.0
ν_7	CF_2 wag	b_{2u} (b_{1u})	405.2
ν_8	CF_2 wag	b_{3g} (b_{2g})	509.8
ν_9	CF_2 asym stretch	b_{3u} (b_{2u})	1340.0[c]
ν_{10}	CF_2 rock	b_{3u} (b_{2u})	209.7[b]
ν_{11}	CF_2 sym stretch	b_{1u} (b_{3u})	1187.6[c]
ν_{12}	CF_2 scissor	b_{1u} (b_{3u})	555.3

[a]Symmetry types refer to a D_{2h} molecule with z axis along the CC bond and the y axis perpendicular to the plane, as used in ref 1 for easier comparison with the C_{2v} symmetric $^{12}C^{13}CF_4$; the more conventional designation[5,24] with x axis along the CC bond and z axis perpendicular to the plane is given in parentheses. [b]Revised value (instead of 210 cm^{-11}), based on a more definite assignment of a hot-band structure and $x_{10,10}$, see Supporting Information. [c]Band origins from high-resolution spectra;[25] low-resolution values are 1338.4 and 1187.0.

For levels involving more than two quanta of vibration, anharmonic shifts are generally additive. This helped to decide between different assignments of combination bands in a few cases where the harmonic sums were similar to each other. However, such additivity need not apply when the levels involved are subject to Fermi resonance, producing shifts that depend on the separation of nearby interacting levels. We use eqs 1−3 to obtain the experimental values, and hence, Table 2 reports phenomenological x_{ij}, some of which show a spread in the values suggestive of Fermi resonances (in particular x_{18}, x_{26}, and x_{77}). Fermi resonances can also be recognized if the apparent x_{ij} or the hot-band structure depends on the isotopologue. For C_2F_4, Fermi resonances were identified (see section 4.4 and SI) between:

- ν_5 and $\nu_2+\nu_6$ (discussed already in ref 1),
- ν_1 and $\nu_5+\nu_6$ (indicated by the hot-band structure of ν_1-combinations, which are different in the mixed isotopologue),
- ν_2 and $2\nu_7$ (causing irregularities in overtone levels of ν_7, also contributing to the large magnitude of x_{27} and x_{77}).
- ν_2 and $2\nu_3$, identified from the MP2 calculations.

The MP2/cc-pVTZ calculations reproduced the observed wavenumbers and isotopic shifts very well.[1] Supporting the overall vibrational analysis, most of the anharmonic x_{ij}

dx.doi.org/10.1021/jp500811w | J. Phys. Chem. A 2014, 118, 5391−5399

Table 2. Anharmonic Constants x_{ij} (in cm^{-1}) of $^{12}C_2F_4$[a]

	1	2	3	4	5	6
1	−7.83					
2	−3.1	−3.8				
	−3.04	−0.62				
3			+0.05			
	−1.93	−0.22	(+0.03)			
4	−1.5	−0.7, −0.3	+0.9	+0.8		
	−1.14	−0.24	−0.22	−0.03		
5			−1.5	−3.2		
	−8.85	(+8.49)	−1.86	−0.69	−2.06	
6	−5.0	−10.85, −8.7	+2.0	−1.1		−0.95
	−4.54	−13.35	−0.07	−0.82	(+10.88)	−0.002
7	−4.6, −3.8	−9.5, −10.1	−1.4	+0.3		−0.7
	−3.27	−9.18	−0.44	(+0.24)	−2.16	−0.78
8	−18.5 or −19.65	−1.32	+0.4	−1.05, −0.7		−4.9, −2.3
	−18.27	−3.08	(+0.24)	−0.75	−4.73	(+0.10)
9	−3.3	−2.0		−0.9	+0.2	−2.75
	−3.78	−4.02	−1.72	−0.85	−11.89	−2.52
10	−1.04	+0.9, +1.0	−1.75	−1.3	−1.2 or **−1.5**	−0.1
	−1.27	−0.39	−0.26	−0.03	−2.86	−0.16
11	−4.6	−1.5	−2.3	−0.7, −0.25	+4.9	−1.4
	−4.56	−3.32	−1.44	−0.52	−6.14	−0.98
12	−0.4	+0.6	+0.85	+0.25		
	(+0.13)	(+0.04)	(+0.05)	−0.10	−3.81	−0.36
	7	8	9	10	11	12
7	+4.1					
	(+2.38)					
8	−1.6, −1.5	+0.05				
	−1.24	(+2.04)				
9	−2.0					
	−2.03	−3.82	−2.68			
10	+0.3	−0.7	−1.2−1.5	+1.25		
	(+0.39)	−0.40	−1.50	(+0.99)		
11	−1.15	−0.7		−0.7	−1.6, −0.45	
	−0.81	−0.13	−6.48	(+0.96)	−1.74	
12	−0.25	+0.5		−0.2		+0.33
	−0.08	(+1.02)	−3.17	(+0.48)	−3.81	(+0.12)

[a]Upright: Experimental values. In parentheses: Values calculated by MP2/pVTZ. Where two values or a range are given for the experimental data, it may indicate (a) a dependence of the effective x_{ij} on the involved levels due to perturbations (Fermi resonances, section 4.4) or (b) an uncertainty due to error limits (e.g., where broad bands are involved) or an uncertain assignment. A preferred value is indicated by bold face. For further details on the derivation of each x_{ij} and some isotopic data, see the Supporting Information.

Scheme 1. Vibrational Modes of C_2F_4; Symmetry Types As Explained for Table 1

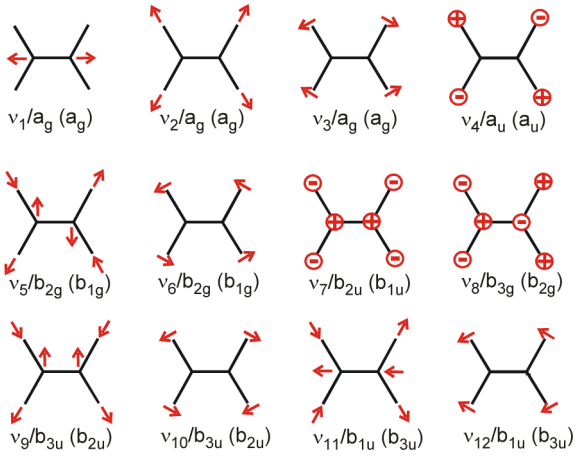

constants of Table 2 also agree well. Exceptions are 15 (x_{22}, x_{28}, x_{29}, $x_{2,10}$, $x_{2,11}$, x_{36}, $x_{3,10}$, x_{45}, x_{59}, $x_{5,11}$, x_{66}, x_{68}, x_{77}, x_{88}, $x_{10,11}$) out of 54 cases where an observed value is available for comparison. Some of these will be discussed below. Most deviations can be attributed to specific Fermi resonances (section 4.4).

4. DISCUSSION

As already described in the Introduction, the peculiar reactions of C_2F_4 have to do with CC stretching and carbon pyramidalization. The discussion will focus on these coordinates (sections 4.1−4.3).

4.1. Dissociation. For a planar geometry, CC dissociation correlates C_2H_4 and C_2F_4 with a pair of carbenes in their lowest triplet states[11] (Figure 2a). Because the energy of forming these products is practically the same for the two molecules, one could also expect that the potential energy curves coincide and the CC stretch force constants are equal. In fact, already early force-field calculations showed no substantial difference (889 N/m for C_2F_4[26] and 940 N/m for C_2H_4[27,28]). Furthermore, the

dx.doi.org/10.1021/jp500811w | J. Phys. Chem. A 2014, 118, 5391−5399

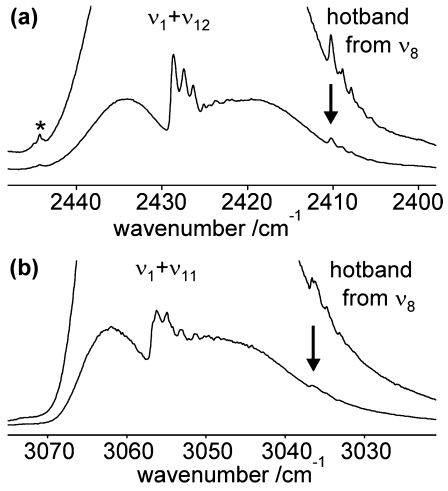

Figure 1. Absorbance spectra demonstrating the large x_{18} derived shifts for hot-bands originating in ν_8. Note the very similar hot-band substructure. (a) $\nu_1+\nu_{12}$, (b) $\nu_1+\nu_{11}$. The $\nu_5+\nu_6+\nu_{12}$ band is marked with an asterisk (*). The spectra were recorded in the Garching laboratory, with pressure and path length of 2 bar and 10 cm (for the lower trace of each panel), and 140 mbar and 4 m (upper trace), respectively.

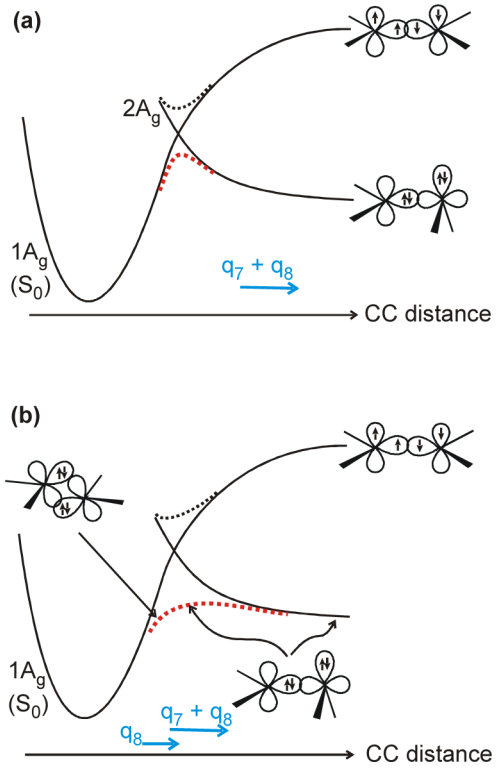

Figure 2. Potentials for ground-state CC dissociation of C_2F_4, leading over an avoided crossing to two singlet carbenes. In (a) it is assumed that the one-sided pyramidalization (q_7 + q_8) begins only after overcoming the barrier, whereas (b) shows the preferred path, where this distortion is already fully developed on the barrier and is preceded by a trans pyramidalization (q_8), while the CC distance is steadily increasing.

short CC distance (132 pm, which is 1 pm shorter than in ethylene[1]) and the high CC stretch wavenumber (1873.8 cm^{-1}, compared to 1625.4 cm^{-1} [29] for ethylene) do not point to a weakened bond. As early as 1965, the low dissociation energy of C_2F_4 was attributed to switching over to a channel producing two singlet carbenes and to the stabilization (by 2.458 eV,[14,15] see Introduction) of singlet CF_2 by back bonding, so that this channel is energetically favored[11] by 4.9 eV. This path hence leads over an avoided crossing of potential surfaces (Figure 2a). If the avoidance is strong, one could expect an influence at least on the anharmonicity x_{11} (ν_1 is dominated by CC stretching), even if not on the force constant at the bottom of the potential energy well. Table 2 shows that the magnitude of x_{11} (calculated −7.8 cm^{-1}) is not unusually large for such a high-frequency vibration, though noticeably larger than for ethylene (x_{22} = −2.3 cm^{-1} [30]). That the increase in magnitude is only moderate can be taken as a sign that the avoidance along this coordinate is not very strong. Hence, the back reaction (recombination) will have a high barrier in planar geometry. Whereas the measured recombination barrier is not, in fact, zero, it is only minor (9 kJ/mol = 0.09 eV [10]). So, a lower-energy path must lead around the barrier, out of the drawing plane of Figure 2a, that is, with distortion different from CC stretch.

It was argued in ref 16 that recombination of two CF_2 molecules should be easiest if one of them points with its filled $n\sigma$ orbital to the empty $p\pi$ orbital of the other. Hence, the dissociation path will change from pure CC stretch to include also pyramidalization (Figure 2b), and the potential should be lowered in energy in the direction of q_7 (the coordinate of ν_7) and/or q_8. In turn, this can affect x_{17} and/or x_{18}. In fact x_{18} has an unusually large magnitude, although x_{17} is in the normal range (Table 2). (The magnitude of x_{18} is not caused by secondary effects such as Fermi resonance, as we shall see in section 4.4.3.) We can conclude that on stretching the CC bond the molecule first bends toward trans pyramidalization (q_8) (Figure 2b). The one-sided nonplanar bending (Figure 2) is a superposition of q_7 and q_8. The reason why q_8 is active earlier than q_7 can be understood by a valence-bond model for weak double bonds.

In this model[12,13,17−19] several symmetric arrangements of carbenes (a−c of Scheme 2) were considered: Whereas with two triplet carbenes all arrangements (a−d) lead to bonding interaction, with two singlet carbenes bonding occurs only in the trans-bent case (c);[17−19] this corresponds to a double donor−acceptor bond. One can add that the cis-bent case with singlet carbenes would lead only to antibonding (Scheme 2d). Malrieu and Trinquier derived a criterion for trans-bending (deriving even the angle) by comparing the standard double-bond energy with the singlet−triplet energy splitting in the carbene fragments.[17,18] Their findings were confirmed by many examples, in particular with heavier-element homologues.[19] We can apply this rule not only to the equilibrium geometry of C_2F_4 but also to its dissociation path, if we consider in the comparison the double-bond energy that is reduced on extension of this bond. The rule thus predicts that on CC extension C_2F_4 is distorted from planar geometry to a trans-bent structure, and this rationalizes the large magnitude of x_{18}.

More recently, Borisov et al. found evidence for trans pyramidalization on extension of the CC bond also from molecular orbital calculation (at high level: Møller−Plesset perturbation theory of second, third and fourth order):[31] The authors found that the onset is relatively sudden on CC extension to 142 pm and that the distortion lowers the energy appreciably. (The large x_{18} anharmonicity is an indication that this pyramidalization already begins not far from the S_0 minimum. In fact, a CC stretch by 10 pm—from 132 to 142

dx.doi.org/10.1021/jp500811w | J. Phys. Chem. A 2014, 118, 5391−5399

Scheme 2. Orbital Interaction in Recombination of Two Triplet or Singlet Difluorocarbenes in Various Geometric Arrangements[a]

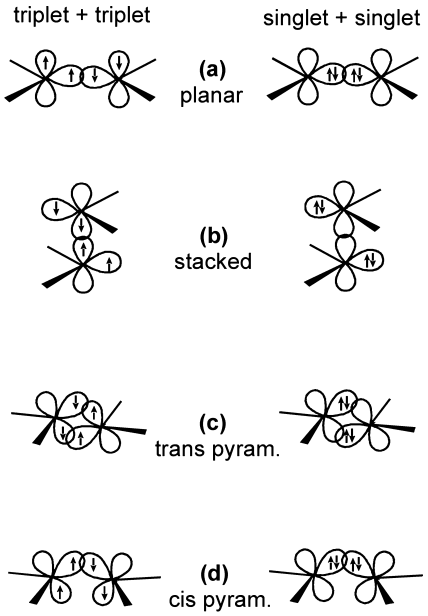

[a]In the triplet case, the interaction can be bonding in all arrangements. In the singlet case, (a) is antibonding, (b) nonbonding, (c) bonding, (d) antibonding. Antibonding arrangements correlate with high-energy states of C_2F_4.

pm—is just about the vibrational amplitude in the $\upsilon_1 = 1$ level.) Although Borisov et al. did not find an energy minimum with such a distortion, they suggested that it plays a crucial role in the low-energy real intermediate found by Buravtsev, Kolbanovskii et al. in thermal reactions of C_2F_4 and recombination of CF_2 (see ref 31 and literature quoted therein and section 4.3).

One could suppose that in order to lower the activation energy for dissociation the only necessary deviation from simple CC stretching is distortion toward the ν_8 coordinate (q_8). The extrapolation of the mentioned calculation suggested just that.[31] However, there is experimental evidence that the asymmetric pyramidalization (corresponding to superposition of q_7 and q_8 as in Figure 2b) is already crucial in the transition state: The pre-exponential factor found in the rate of thermal C_2F_4 dissociation (2.8×10^{15} s^{-1} [10]) is clearly larger than would be typical for a simple bond splitting (10^{13} s^{-1}). This corresponds to a raised entropy of activation, such as that which happens if an additional degree of freedom is activated in the transition state. The most plausible candidate is free internal rotation, as it can be expected in the asymmetric structure with a single dative bond but not in symmetric geometry with double donor—acceptor bond. This picture is also consistent with a stepwise cleavage of the double donator—acceptor bond on C_2F_4 dissociation and its stepwise formation on CF_2 recombination.

It is worth noting that the molecule with one-sided pyramidalization has an electron distribution (Figure 2b) that is zwitterionic and correlates in planar geometry with the $2A_g$ state with two π electrons excited to π^*, as already pointed out in ref 16.

A fully analogous dissociation path can also be expected for the other systems considered by Malrieu and Trinquier. In fact, according to ref 32 ground-state (IR induced) dissociation of diazomethane (H_2CNN) follows a path with a pyramidalized methylene group to produce N_2 + singlet CH_2; the out-of-plane deformation was experimentally confirmed. In the backward reaction, N_2 points with its $n\sigma$ electron pair to the empty $p\pi$ orbital of the singlet methylene (see refs 32 and 33 for a calculated potential in two dimensions, which would look similar for C_2F_4). The potential is also similar to that of the isoelectronic ketene.[34] Hence, the out-of-plane deformation on dissociation of C_2F_4 is not an isolated phenomenon.

4.2. Force Constants of Wagging (pyramidalization, ν_7 versus ν_8). Applying their energetic criterion to the equilibrium geometry of C_2F_4, Trinquier and Malrieu found that this molecule is not far from the limit, where it would become nonplanar, and suggested that the ν_8 force constant may be significantly lower than that of ethylene.[18] This is in fact confirmed in the following way: Analytical expressions for a valence force field model for planar X_2Y_4 were given by Herzberg.[24] Besides the masses m_X and m_Y, bond lengths l_1 (for XX) and l_2 (XY) and the angle α (half of YXY), both ν_7 and ν_8 only depend on the force constant for pyramidalization (k_β/l_2^2). With equilibrium distances and angles from ref 1 and $\lambda_i = (2\pi c\nu_i)^2$ one derives this force constant from ν_7 and ν_8 (with identical results for $^{12}C_2F_4$ and $^{13}C_2F_4$):

$$\frac{k_\beta}{l_2^2} = \lambda_7 2\cos^2\alpha \; m_Y\left(1 + 2\frac{m_Y}{m_X}\right)^{-1} = 26.8\,\mathrm{N/m}$$

$$\frac{k_\beta}{l_2^2} = \lambda_8\cos^2\alpha \; m_Y\left(1 + \frac{m_Y}{m_X}\left(1 + 2\frac{l_2}{l_1}\cos\alpha\right)^2\right)^{-1} = 11.2\,\mathrm{N/m} \quad (4)$$

Both values should be identical in this valence-force field model. In fact for ethylene, the value is 22.9 N/m,[24] whether derived from ν_7 or ν_8. The pyramidalization force constant derived from ν_7 of C_2F_4 is slightly higher than in ethylene (by 17%), but the same quantity derived from ν_8 is only 49% of the ethylene value. (Of course, these values are not quantitatively meaningful, as the discrepancy highlights that a pure valence-force field model is not sufficient for wagging of C_2F_4.) So in fact the restoring force for the ν_8 vibration is significantly smaller than in ethylene and than that expected on the basis of the same pyramidalization force constant as for ν_7. This is consistent with the prediction of the valence-bond model favoring the trans-bent geometry.

The slightly raised force constant for ν_7 could be due to repulsive nonbonding interaction in cis pyramidalization. Such a geometry would be involved in the hypothetical transition state of the Diels—Alder addition of C_2F_4 to butadiene, a reaction that has not been observed. It was argued that an increased energy associated with this distortion might contribute to inhibiting the reaction.[7] However, an increase in the force constant of only 17% is hardly sufficient to support this explanation, and the other effects discussed in ref 7, in particular the competing fast radical reactions, are probably more important.

4.3. Torsion (ν_4). Applying again the force-field formulas of Herzberg,[24] the force constant for torsion, k_γ/l_2^2, is found to be 30.3 N/m for both ethylene and tetrafluoroethylene. That is, near the potential minimum the C=C bond in C_2F_4 behaves just like a normal double bond. Consequently, the torsional barrier at a 90° twist (which is a measure of the π bond strength) would be identical for both molecules (2.8 eV) if the

dx.doi.org/10.1021/jp500811w | J. Phys. Chem. A 2014, 118, 5391−5399

Table 3. Calculated (MP2/cc-pVTZ) and Experimental Anharmonic Constants x_{ij} (in cm^{-1}) That Show Significant Isotopic Differences

	x_{18}	x_{25}	x_{26}	x_{27}	x_{45}	x_{56}	x_{59}	$x_{5,11}$	x_{77}
calculated									
$^{12}C_2F_4$	−18.3	+8.49	−13.4	−9.18	−0.69	+10.9	−11.9	−6.14	+2.38
$^{13}C_2F_4$	−16.8	−16.0	+11.2	−13.9	−0.66	−13.7	−11.2	−5.58	+3.55
difference	1.42	−24.5	+24.6	−4.73	0.03	−24.6	0.7	0.56	1.17
experimental									
$^{12}C_2F_4$	−19.0		−10.85	−9.5	−3.2		+0.2	+4.9	+4.1
$^{13}C_2F_4$	−16.6		∼+5.0	−10.0	−2.3		−1.0	+4.0	+8.1
difference	2.4		15.8	−0.5	0.9		−1.2	−0.9	4.0
influenced by	FR3	FR2	FR1, FR2	FR1	FR2	FR2, FR3	FR2	FR2	FR1
Fermi Resonances (FR)									

Interacting levels with their harmonic positions and anharmonic shifts (cm^{-1}) are indicated; the calculations in this section support the larger FR1-shift (16.3) for the heaviest isotopologue.

FR1: ν_2 / $2\nu_7$, $^{12}C_2F_4$: 776.1/810.4 + 8.2, $^{12}C^{13}CF_4$: 773.5/797.6 + 10.9, $^{13}C_2F_4$: 769.7/786.8 + (14.5...16.3)

FR2: ν_5 / $\nu_2+\nu_6$, $^{12}C_2F_4$: 1337.7/1326.6 − (8.7...10.8), $^{13}C_2F_4$: 1285.6/1316.7 − 7.7

FR3: ν_1 / $\nu_5+\nu_6$, $^{12}C_2F_4$: 1873.8/1887.7 + (10.9 calc.), $^{13}C_2F_4$: 1806.3/1832.8− (13.7 calc)

FR4: ν_2 / $2\nu_3$, $^{12}C_2F_4$: 776.1/790.2 + 0.1, $^{13}C_2F_4$: 769.7/790.0 + (0.1)

FR5: $\nu_3/2\nu_{10}$, $^{12}C_2F_4$: 395.1/419.4 + 2.5, $^{13}C_2F_4$: 395.0/418.0 + (2.5)

two C−CF_2 groups remained planar; this was confirmed by a high-level calculation.[8] However, pyramidalization lowers this barrier by 0.57 eV (at MP2 level,[8] consistent with ref 35). If this stabilization is activated early along q_4, it could give rise to substantially negative values for x_{44} and especially for x_{47} and x_{48}. However, x_{44} and x_{47} are actually slightly positive (0.8 and 0.3 cm^{-1}) and x_{48} has no unusual magnitude (−0.7 to −1.05 cm^{-1}). Evidently, the stabilizing effect of pyramidalization becomes effective only at high torsional angles. The corresponding values for ethylene are −2.4, −8.9, and −7.2 cm^{-1}, respectively.[30]

The nondiagonal anharmonicities x_{i4} and x_{4j} are generally smaller in magnitude than in ethylene. But this may simply have to do with the relative vibrational amplitudes, which are much larger for torsion of CH_2 than of CF_2 due to the relative masses.

In the twisted-pyramidalized structure of C_2F_4, the triplet (T_1) is only 0.013 eV lower than the singlet (S_0).[8] In contrast to S_0, T_1 has an energy minimum at this geometry. It can therefore act as a real intermediate and undergo radical-type reactions, further assisted by its low energy that is calculated at 2.1 eV.[8,35] This has been a widespread interpretation of some peculiarities of C_2F_4 reactions (see, for example ref 7). However, Buravtsev, Kolbanovskii et al. found in shock-tube experiments (with C_2F_4 diluted by Ar and adiabatically compressed) an intermediate at much lower energy (0.8 to 1 eV) with UV and visible absorption (235 and 500 nm) (see refs 31,36, and 37 and the literature quoted there). They supposed it to be a singlet diradicaloid of C_2F_4 with a geometry corresponding not to an energy minimum but to a point on a slope of the potential (see, for example ref 31). However, as these points are not stationary there are too many (nearly) isoenergetic locations with shifted electronic transitions, so that the electronic absorption would be smeared out. It was therefore suggested[16] that the observed intermediate is another low-energy isomer, tetrafluoro-ethylidene CF_3CF (electronic absorption in an Ar matrix:[38]). However, its energy (1.9 eV [39]) seems to be nearly as high as that of the twisted-pyramidalized triplet. Hence, the identity of the observed intermediate is still unclear. (In one study the twisted-pyramidalized C_2F_4 triplet is calculated at 0.90 eV,[40] but computational details are not given, and previous theoretical results are not discussed.)

4.4. Other Anharmonicities, Fermi Resonances and Isotope Effects. Some more anharmonicities of Table 1 have unusually large magnitudes or show a range of values and/or deviate from prediction. In many of them Fermi resonances play a role, as will be explained here. In section4.4.3, however, it is shown that x_{18} is hardly influenced by such effects and its large magnitude mainly results from the overall shape of the potential energy surface.

Fermi resonances[24,41] mix two nearby levels of the same symmetry, which differ by three units in the quantum numbers. Examples are the pairs $\nu_2/2\nu_7$ and $\nu_5/\nu_2+\nu_6$. The Fermi-induced repulsion of the levels depends in a nonlinear way on both the magnitude of the Fermi interaction parameter and on the original (i.e., unperturbed) energetic distance of the levels. This separation will, in general, change (a) on isotopic substitution and (b) on adding a quantum of another vibration (i.e., in analogous combination bands; similarly also in higher overtones, in which case a quantum number dependence must also be taken into account[24]). Both dependences can be used to recognize Fermi resonances. They imply isotope and level-dependent anharmonic "constants". Another method of characterizing Fermi resonance interactions relies on intensity borrowing caused by the mixing of levels.

According to the MP2 calculations, the great majority of x_{ij} change by $\ll 1$ cm^{-1} on isotopic substitution. The few exceptions are listed in Table 3 and are compared to experimental values. Identified (FR1−3) and potential Fermi resonances are also listed. The interpretation in the line "influenced by" is based on the assumption that an x_{ij} is affected by such a resonance if at least one of the levels ν_i and ν_j is involved in the Fermi interaction.

The table shows that the calculated isotopic shift is sometimes much larger than in the experiment, for instance x_{26}, x_{27}. Also x_{56} for $^{12}C_2F_4$ is probably too large, as the two observed bands $\nu_5+\nu_6+\nu_{11}$ and $\nu_5+\nu_6+\nu_{12}$ are close to their harmonic positions (Table S1 in SI). It seems that at the present level of theory, the calculation does not reliably reproduce the Fermi resonance induced shifts, at least the stronger ones. This is not surprising given the highly sensitive and nonlinear dependence of Fermi shift on the "unperturbed" level separations. The same deficiency will also affect those x_{ij}

dx.doi.org/10.1021/jp500811w | J. Phys. Chem. A 2014, 118, 5391−5399

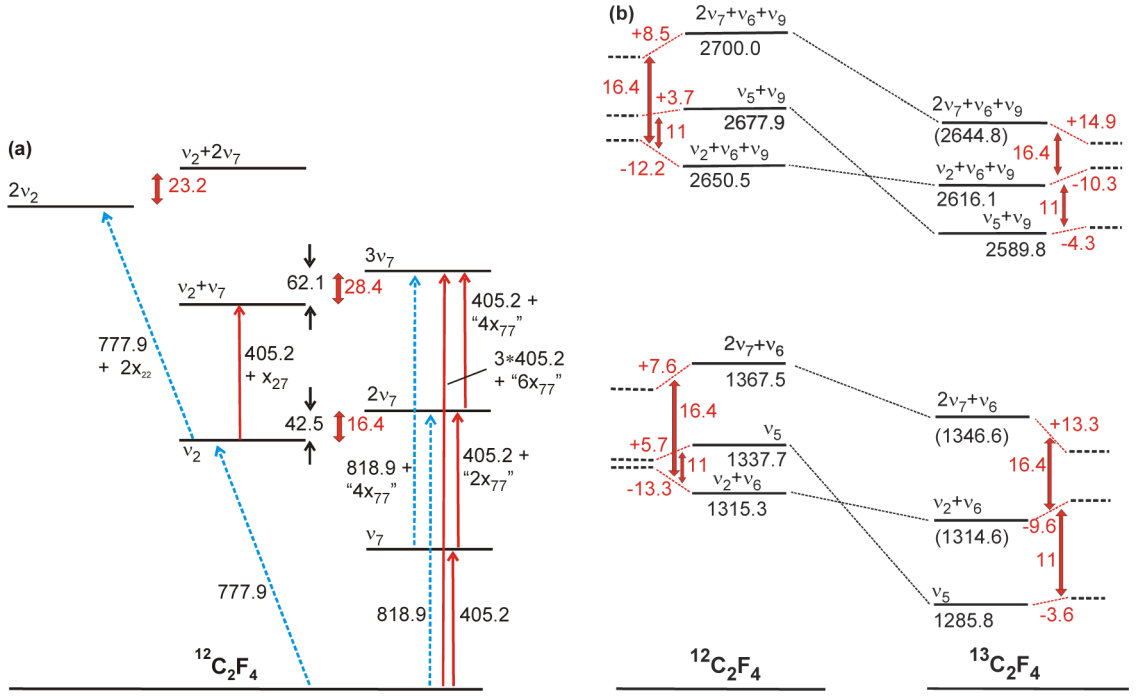

Figure 3. Some levels involved in Fermi resonances and observed transitions. Solid arrows: IR, broken arrows: Raman;[2] double arrows (with interaction matrix element) indicate repulsion between level pairs. Numbers are in cm^{-1}. (a) $\nu_2/2\nu_7$ Fermi resonance in $^{12}C_2F_4$. The anharmonic shifts involving x_{77} are only nominal, because the Fermi perturbation is strong: "$6x_{77}$" =18.1 is less than 3 times "$2x_{77}$" (= 8.2) and "$4x_{77}$" is only 9.9. (But "$2x_{77}$" + "$4x_{77}$" = "$6x_{77}$", as is obvious from the level scheme, and the Raman anharmonic shifts practically coincide with those from the IR spectra.) (b) Three-level Fermi resonance $\nu_5/\nu_2+\nu_6/2\nu_7+\nu_6$ and their combinations with ν_9 for $^{12}C_2F_4$ and $^{13}C_2F_4$. The indicated level energies are from the spectra except those in parentheses, which are calculated. The broken horizontal lines are the estimated unperturbed positions (see the SI), and the signed numbers are the calculated shifts.

connected with at least one level (or a combination thereof) involved in a resonance listed above (examples in Figure 3a). In fact, 10 of the 15 deviations listed at the end of section 3 can be attributed in this way to the resonances FR1 and FR2 with possible contributions of FR3. The exceptions are x_{36}, $x_{3,10}$, x_{66}, x_{68}, and x_{88}. In all 42 other cases the agreement between calculated and spectral values can be considered good to excellent.

It is worthwhile to consider the two strongest Fermi resonances, FR1 ($\nu_2/2\nu_7$) and FR2 ($\nu_5/\nu_2+\nu_6$), in $^{12}C_2F_4$ in some detail. The effect of these resonances is summarized in Figure 3.

4.4.1. The $\nu_2/2\nu_7$ Resonance. The scheme in Figure 3a shows levels influenced by FR1. The 16.4 cm^{-1} magnitude of the interaction term (with its expected dependence on quantum numbers[24]) has been derived from band shifts and intensities for a series of levels built on $\nu_2/2\nu_7$ for all three isotopologues. Bands for $2\nu_7+\nu_x$ (x = 9, 11) borrow their entire intensity from $\nu_2+\nu_x$. The detailed analysis is provided in SI. Quite a number of transitions can be consistently assigned (Figure 3a). It is also evident that x_{77}, x_{27} and x_{22} are affected by the Fermi resonance (and probably other x_{2i}, if the level separations differ) and that x_{77} is level dependent because of the varying separation. The Fermi term is almost entirely responsible for the +8.2 cm^{-1} shift of $2\nu_7$ for $^{12}C_2F_4$ and those of the heavier isotopologues (Table 3 under FR1). In the latter the Fermi-induced shift is increased, because the levels ν_2 and $2\nu_7$ (before perturbation) are closer together than in $^{12}C_2F_4$ and are practically degenerate in $^{13}C_2F_4$. The success of these calculations shows that the additional mixing of ν_2 with $2\nu_3$ (FR3) is apparently a weak perturbation at most.

4.4.2. The Simultaneous $\nu_5/\nu_2+\nu_6$ and $\nu_2+\nu_6/2\nu_7+\nu_6$ Interactions. The Fermi resonance FR2 between ν_5 and $\nu_2+\nu_6$ was qualitatively discussed in ref 1. A more complete understanding of the resonance shifts and pattern of intensity borrowing requires the three-level scheme shown in Figure 3b; this figure also shows combinations with ν_9, as they are all IR active and were directly observed. Analysis based on this model has enabled the magnitude of the Fermi term to be determined as 11 cm^{-1}; the FR1 term of 16.4 cm^{-1} was used without change. Again, the details are provided in SI. Significantly, the model predicts varying FR shifts that even differ in sign (originating from the different repulsions in Figure 3b) and can thus account for the unusual isotopic shifts observed between $^{12}C_2F_4$ and $^{13}C_2F_4$. It explains a substantial deviation of the observed isotopic shift $\Delta\nu_5 = -51.9$[1] from the value of $\Delta\nu_5{}^0 = -43.1$ expected from the Teller–Redlich product rule, which is valid for harmonic oscillators.[24] Additionally the relative intensities of combination bands and their isotopic dependence are well predicted. It is also remarkable that according to the model the largest part of the anharmonicity x_{26} is due to Fermi resonance.

As described in ref 1, the lower symmetry in $^{12}C^{13}CF_4$ leads to strong mixing of ν_5 with ν_9 (which are nearly degenerate in $^{12}C_2F_4$). The two levels repel each other (even in the harmonic approximation) and give rise to two infrared-active transitions. It is sometimes difficult to disentangle them and their combination bands from the spectra. Furthermore, the Fermi resonance scheme will become yet more complicated. We therefore did not try to analyze it in the mixed isotopic species.

4.4.3. Is the Magnitude of x_{18} Caused by $\nu_1/\nu_5+\nu_6$ Fermi Resonance? If the large magnitude of some anharmonicities is

dx.doi.org/10.1021/jp500811w | J. Phys. Chem. A 2014, 118, 5391–5399

caused by Fermi resonance, a crucial question is whether this might also be the case for x_{18}. If so, the conspicuous value of x_{18} could be largely a matter of the character of the resonance and less a consequence of global features of the potential for dissociation, which we considered in section 4.1. In fact, weak perturbations of the ν_1 level and its combinations by the $\nu_1/\nu_5+\nu_6$ Fermi resonance are indicated by the slight x_{18} dependence on the level and on isotopic substitution and the change of the hot-band structure of ν_1 combinations in $^{12}C^{13}CF_4$, as explained in the SI.

A quantitative estimate of the strength of the $\nu_1/\nu_5+\nu_6$ interaction can be deduced from the intensities of $\nu_5+\nu_6$ combinations relative to those of the corresponding ν_1 combinations, assuming that the former borrow their full strength from the latter. The $\nu_5+\nu_6+\nu_{12}$ band (2444.3 cm^{-1}) has ~1−2% the strength of the $\nu_1+\nu_{12}$ band (2428.7 cm^{-1}), see Figure 1a. Similarly, the $\nu_5+\nu_6+\nu_{11}$ shoulder (3072 cm^{-1}) is <1% as intense as $\nu_1+\nu_{11}$ (3056.2 cm^{-1}) and clearly visible only with longer path length than shown in Figure 1b. From both observations, one can estimate a Fermi term (W) of no more than ~2.5 cm^{-1}, causing a shift (and consequent change in x_{18}) of <0.5 cm^{-1}. This is actually an upper bound, because such weak bands can also be expected without intensity borrowing. Hence, Fermi resonance affects the magnitude of x_{18} only by a little (by <3%), and we can maintain the conclusions of section 4.1 on the shape of the potential.

5. CONCLUSION

A large set of anharmonic constants of C_2F_4 was derived from spectroscopic data, and a complete set was calculated. Most of the calculated and experimental values agree very well, and nearly all deviations can be attributed to Fermi resonances. The values were used to interpret peculiarities of the potential and reactions of this molecule.

The facile thermal CC dissociation of C_2F_4 is due to curve crossing of the ground state ($1A_g$) with the two-electron excited zwitterionic $2A_g$ state. The crossing barely alters the properties of the potential curve (cut purely as a function of CC stretch) near the equilibrium geometry; the force constant for CC stretching (ν_1 in C_2F_4, ν_2 in C_2H_4) is nearly identical for the two molecules. Only a slightly larger magnitude of the anharmonicity x_{11} compared to the corresponding x_{22} of ethylene provides a hint of a weakly avoided crossing in planar geometry of C_2F_4.

However, the large magnitude of x_{18} leads us to conclude that the dissociation path bends early toward q_8, i.e. to trans pyramidalization of the two carbon atoms (Figure 2b). This is rationalized by a valence-bond model, which describes the stretched CC bond as a double donor−acceptor bond (Scheme 2c). It is also consistent with the tendency of fluorine to induce sp^3 hybridization at carbon, although this preference alone would also allow cis pyramidalization, q_7, which is not involved early in dissociation. On further CC stretching, one of the two donor−acceptor bonds breaks, and the pyramidalization becomes fully one-sided already in the transition state (Figure 2b). In this way, free internal rotation of the CF_2 groups becomes possible, providing an additional degree of freedom that rationalizes the high pre-exponential factor in the rate constant of dissociation. This structure with perpendicular arrangement of the two CF_2 groups appears very plausible for the back reaction. Thus, one CF_2 group approaches with its filled nσ orbital the empty pπ orbital of the other CF_2 group (Figure 2b). The easy trans pyramidalization on minor CC stretching is probably also the reason that the corresponding ν_8 force constant is lowered, although all other force constants are similar to those in ethylene.

The preference of fluorine for sp^3 hybridization at carbon has been invoked to explain not only the easy radical addition and other reactions, but also the low-lying, twisted-pyramidalized triplet, which is nearly isoenergetic with the singlet that has a saddle point there. However, it seems that pyramidalization begins only at high torsional angles. This is indicated by x_{44}, x_{47}, and x_{48}, which have no unusual values.

Very recently, high-level theoretical studies[42] investigated electronic ground and excited states of C_2F_4 and their dependence on some coordinates, mainly to discover the fate of this molecule after electronic excitation and make comparisons with a corresponding time-resolved experiment (ref 16). For the ground state, the stabilizing effect of pyramidalization in the twisted molecule was confirmed. Interestingly, the excited molecule enters the S_1/S_0 conical intersection from the $2A_g$ state, where the molecule has a large one-sided pyramidalization, a 90° CC twist and a CC bond length (1.51 Å) similar to that of a single bond. In the present work, the transition state for S_0 dissociation was said to result from avoided crossing of the $2A_g$ and $1A_g$ (i.e., S_0) states, also with large one-sided pyramidalization but at longer CC distances and perhaps without twist. It would be interesting to check whether these geometrical differences are large enough to generate an excited-state barrier, because evidence was found in ref 16 that CC dissociation does not begin in the excited state.

■ ASSOCIATED CONTENT

Ⓢ Supporting Information

Observed infrared bands with their assignment, the sources of anharmonic constants, an analysis of Fermi resonances, additional spectra and a full list of the authors of ref 22. This material is available free of charge via the Internet at http://pubs.acs.org.

■ AUTHOR INFORMATION

Corresponding Authors

*E-mail: w.fuss@mpq.mpg.de (W.F.)
*E-mail: E.Robertson@latrobe.edu.au (E.R.)

Present Addresses

[&]Weidachstr. 12, 85748 Garching, Germany.
[⊥]Max-Planck-Institut für Struktur und Dynamik der Materie, 22761 Hamburg, Germany.

Notes

The authors declare no competing financial interest.

■ ACKNOWLEDGMENTS

The support of the Australian Synchrotron through beam-time access and of Australia's NCI Facility through the National Computational Merit Allocation Scheme to perform quantum chemical calculations is gratefully acknowledged.

■ REFERENCES

(1) Medcraft, C.; Fuß, W.; Appadoo, D. R. T.; McNaughton, D.; Thompson, C. D.; Robertson, E. G. Structural, Vibrational and Rovibrational Analysis of Tetrafluoroethylene. *J. Chem. Phys.* **2012**, *137*, 214301/1−11.

(2) Nielsen, J. R.; Claassen, H. H.; Smith, D. C. Infrared and Raman Spectra of Fluorinated Ethylenes. 3. Tetrafluoroethylene. *J. Chem. Phys.* **1950**, *18*, 812−817.

(3) Mann, D. E.; Acquista, N.; Plyler, E. K. Vibrational Spectra of Tetrafluoroethylene and Tetrachloroethylene. *J. Res. Natl. Bur. Stand., Sect. A* **1954**, *52*, 67−72.
(4) Monfils, A.; Duchesne, J. The Raman Spectrum of Tetrafluoroethylene in the Condensed Phase, with Further Assignments of the Fundamental Frequencies. *J. Chem. Phys.* **1950**, *18*, 1415.
(5) Shimanouchi, T. *Tables of Molecular Vibrational Frequencies*; National Bureau of Standards: Washington DC, 1972, Vol. *1*.
(6) Getty, S. J.; Borden, W. T. Why Does Tetrafluoroethylene Not Undergo Diels-Alder Reaction with 1,3-Butadiene? An Ab Initio Investigation. *J. Am. Chem. Soc.* **1991**, *113*, 4334−4335.
(7) Borden, W. T. Effects of Electron Donation into C-F σ^* Orbitals: Explanations, Predictions and Experimental Tests. *Chem. Commun.* **1998**, 1919−1925.
(8) Wang, S. Y.; Borden, W. T. Why Is the π Bond in Tetrafluoroethylene Weaker Than That in Ethylene? An Ab Initio Investigation. *J. Am. Chem. Soc.* **1989**, *111*, 7282−7283.
(9) Margrave, J. L.; Wieland, K. Equilibria Involving the CF(g) and CF_2(g) Radicals at High Temperatures. *J. Chem. Phys.* **1953**, *21*, 1552−1554.
(10) Schug, K. P.; Wagner, H. G. Der thermische Zerfall von C_2F_4 in der Gasphase. Zur Bildungsenthalpie von Difluorcarben. *Ber. Bunsenges. Phys. Chem.* **1978**, *82*, 719−725.
(11) Simons, J. P. Chemical Behaviour of Difluorocarbene, and the Dissociation of the Carbon-Carbon Bond in Tetrafluoroethylene. *Nature* **1965**, *205*, 1308−1309.
(12) Carter, E. A.; Goddard, W. A., III. Relation between Singlet-Triplet Gaps and Bond Energies. *J. Phys. Chem.* **1986**, *90*, 998−1001.
(13) Carter, E. A.; Goddard, W. A., III. The C═C Double Bond of Tetrafluoroethylene. *J. Am. Chem. Soc.* **1988**, *110*, 4077−4079.
(14) Koda, S. Emission and Energy Transfer of Triplet Difluoromethylene Produced in the Reaction of Oxygen Atoms with Tetrafluoroethylene. *Chem. Phys. Lett.* **1978**, *55*, 353−357.
(15) Zhou, S.; Zhan, M.; Qiu, Y.; Liu, S.; Shi, J.; Li, F.; Yao, J. Chemiluminescence of $CF_2(^3B_1)$ Produced by the Reaction $O(^3P)$ + C_2F_4. *Chem. Phys. Lett.* **1985**, *121*, 395−399.
(16) Trushin, S. A.; Sorgues, S.; Fuß, W.; Schmid, W. E. Coherent Oscillation and Ultrafast Internal Conversion of Tetrafluoroethylene after Excitation at 197 nm. *ChemPhysChem* **2004**, *5*, 1389−1397.
(17) Malrieu, J. P.; Trinquier, G. Trans Bending at Double Bonds. Occurrence and Extent. *J. Am. Chem. Soc.* **1989**, *111*, 5916−5921.
(18) Trinquier, G.; Malrieu, J. P. Nonclassical Distortions at Multiple Bonds. *J. Am. Chem. Soc.* **1987**, *109*, 5303−5315.
(19) Driess, M.; Grützmacher, H. Main Group Element Analogues of Carbenes, Olefins, and Small Rings. *Angew. Chem., Int. Ed.* **1996**, *55*, 828−856.
(20) Bartlett, P. D.; Dempster, C. J.; Montgomery, L. K.; Schueller, K. E.; Wallbillich, G. E. H. Cycloaddition. 10. Reversibility in the Biradical Mechanism of Cycloaddition. Tetrafluoroethylene and 1,1-Dichloro-2,2-Difluoroethylene with 2,4-Hexadiene. *J. Am. Chem. Soc.* **1969**, *91*, 405−409.
(21) Fuß, W.; Göthel, J.; Ivanenko, M. M.; Schmid, W. E.; Hering, P.; Kompa, K.-L.; Witte, K. Macroscopic Isotope Separation of ^{13}C by a CO_2 Laser. *Isotopenpraxis* **1994**, *30*, 199−203.
(22) Frisch, M. J.; Trucks, G. W.; Schlegel, H. B.; Scuseria, G. E.; Robb, M. A.; Cheeseman, J. R.; Montgomery, J. A., Jr.; Vreven, T.; Kudin, K. N.; Burant, J. C. et al. *Gaussian 03*, Revision C.02; Gaussian: Wallingford CT, 2004.
(23) Dunning, T. H. Gaussian Basis Sets for Use in Correlated Molecular Calculations. I. The Atoms Boron through Neon and Hydrogen. *J. Chem. Phys.* **1989**, *90*, 1007−1023.
(24) Herzberg, G. *Infrared and Raman Spectra of Polyatomic Molecules*; Van Nostrand Reinhold: New York, 1945; Vol. *2*.
(25) Robertson, E. G.; Thompson, C. D.; Appadoo, D.; McNaughton, D. Tetrafluoroethylene: High-Resolution IR Spectroscopy. *Phys. Chem. Chem. Phys.* **2002**, *4*, 4849−4854.
(26) Mann, D. E.; Fano, L.; Meal, J. H.; Shimanouchi, T. Normal Coordinate Analysis of Halogenated Ethylenes. 2. Perhalogenated Ethylenes. *J. Chem. Phys.* **1957**, *27*, 51−59.
(27) Duncan, J. L.; Hamilton, E. An Improved General Harmonic Force Field for Ethylene. *J. Mol. Struct. (THEOCHEM)* **1981**, *76*, 65−80.
(28) Martin, J. M. L.; Lee, T. J.; Taylor, P. R.; François, J. P. The Anharmonic Force Field of Ethylene, C_2H_4, by Means of Accurate Ab Initio Calculations. *J. Chem. Phys.* **1995**, *103*, 2589−2602.
(29) Knippers, W.; van Helvoort, K.; Stolte, S.; Reuss, J. Raman Overtone Spectroscopy of Ethylene. *Chem. Phys.* **1985**, *98*, 1−6.
(30) Duncan, J. L.; Robertson, G. E. Vibrational Anharmonicity in Ethylenic Compounds. *J. Mol. Spectrosc.* **1991**, *145*, 251−261.
(31) Bilera, I. V.; Borisov, Y. A.; Buravtsev, N. N.; Kolbanovskii, Y. A. Tetrafluoroethylene: Spectroscopy and Threshold Quantum Effect. *Dokl. Phys. Chem.* **2002**, *386*, 235−238.
(32) Windhorn, L.; Yeston, J. S.; Witte, T.; Fuß, W.; Motzkus, M.; Proch, D.; Kompa, K. L.; Moore, C. B. Getting Ahead of IVR: A Demonstration of Mid-Infrared Induced Molecular Dissociation on a Sub-Statistical Time Scale. *J. Chem. Phys.* **2003**, *119*, 641−645.
(33) Papakondylis, A.; Mavridis, A. A Theoretical Investigation of the Structure and Bonding of Diazomethane, CH_2N_2. *J. Phys. Chem. A* **1999**, *103*, 1255−1259.
(34) Klippenstein, S. J.; East, A. L. L.; Allen, W. D. A High Level Ab Initio Map and Direct Statistical Treatment of the Fragmentation of Singlet Ketene. *J. Chem. Phys.* **1996**, *105*, 118−140.
(35) Borisov, Y. A. Ab Initio Studies of Tetrafluoroethylene and Tetratrifluoromethylethylene Molecules in the Ground And "Twisted" States. *Russ. Chem. Bull.* **1998**, *47*, 584−586.
(36) Buravtsev, N. N.; Kolbanovsky, Y. A. Intermediates of Thermal Transformations of Perfluoro-Organic Compounds. New Spectral Data and Reactions. *J. Fluorine Chem.* **1999**, *96*, 35−42.
(37) Buravtsev, N. N.; Kolbanovskii, Y. A.; Ovsyannikov, A. A. Biradical Intermediates in Tetrafluoroethylene Dissociation and Difluorocarbene Recombination. *Mendeleev Commun.* **1994**, 190−191.
(38) O'Gara, J. E.; Dailey, W. P. Direct Observation, Reactions under Matrix-Isolation Conditions, and Ab Initio Calculations for Halo-(Trifluoromethyl)Carbenes. Evidence for Photochemical Addition of a Carbene to Dinitrogen. *J. Am. Chem. Soc.* **1992**, *114*, 3581−3590.
(39) Cramer, C. J.; Hillmyer, M. A. Perfluorocarbenes Produced by Thermal Cracking. Barriers to Generation and Rearrangement. *J. Org. Chem.* **1999**, *64*, 4850−4859.
(40) Kalnin'sh, K. K. Thermal Electronic Excitation of Perfluoroolefins. *Russ. J. Appl. Chem.* **2002**, *75*, 589−597.
(41) Califano, S. *Vibrational States*; Wiley: London, 1976.
(42) Mullinax, J. W.; Sokolov, A. Y.; Schaefer, H. F. Conical Intersections and Low-Lying Electronic States of Tetrafluoroethylene. *ChemPhysChem* **2014**, DOI: 10.1002/cphc.201402073.